Article

Not peer-reviewed version

Human BMP4 mRNA Encapsulated in Lipid Nanoparticle Delayed Cartilage Degeneration but Has a Limited Enhancement Effect on Bone Healing in Aged Mice

Xueqin Gao *, Zuokui Xiao, Matthieu Huard, Keisuke Nakayama, Aryn Cummmins, Britney S Force, Hongye Li, Chiara Mancino, John P. Cooke, Francesca Taraballi, Marc J. Philippon, Johnny Huard *

Posted Date: 10 April 2026

doi: 10.20944/preprints202604.0770.v1

Keywords: human BMP4 chemically modified mRNA; critical calvarial bone defect; osteoarthritis; age-related osteoarthritis; lipid nanoparticle; bone tissue engineering

 doi:10.20944/preprints202604.0770.v1

Article

Human BMP4 mRNA Encapsulated in Lipid Nanoparticle Delayed Cartilage Degeneration but Has a Limited Enhancement Effect on Bone Healing in Aged Mice

Xueqin Gao [1,*], Zuokui Xiao [1], Matthieu Huard [1], Keisuke Nakayama [1], Aryn Cummings [2], Britney S Force [1], Hongye Li [3], Chiara Mancino [3], John P. Cooke [3], Francesca Tarabali [3], Marc J. Philippon [1] and Johnny Huard [1,*]

[1] Linda and Mitch Hart Center for Regenerative and Personalized Medicine, Steadman Philippon Research Institute, Vail, CO, USA

[2] Center for Musculoskeletal Regeneration, Houston Methodist Academic Institute; Houston, TX, USA

[3] Laboratory Animal Resources, Colorado State University

* Correspondence: xgao@sprivail.org (X.G.); jhuard@sprivail.org (J.H.)

Abstract

Segmental bone defects and age-related osteoarthritis (OA) are clinically challenging in terms of treatment. Although preclinical studies have demonstrated efficacy for bone defect healing and OA using ex vivo gene therapy or biomaterial sustain-release delivery, few have translated into clinical therapies due to safety concerns. Bone morphogenetic proteins belong to the TGFβ superfamily and are effective in bone and cartilage regeneration/repair. Among BMPs, BMP4 is not only effective in promoting bone and cartilage repair but also promotes stem cell renewal potential and exhibits anti-aging effects. Therefore, the aim of this study is to investigate whether human BMP4 mRNA encapsulated in lipid nanoparticles (hBMP4/LNP) can promote bone and cartilage repair. Our results demonstrated that hBMP4/LNP promoted limited new bone formation only at 2 weeks after creation of defect in critical-sized calvarial bone defect in aged mice at 50μg dose when delivered using fibrin sealant hydrogel as revealed by micro-CT and histology. However, intra-articular injection (IA) of lower doses (2.5 and 5μg) in aged mice knee joints prevented cartilage loss as demonstrated by micro-CT, decreased OARSI histology scores and improved cartilage specific matrix COL2. HBMP4/LNP treatment showed a trend of pain alleviation and did not change serum hyaluronic acid levels. In conclusion, human BMP4 mRNA encapsulated in lipid nanoparticle improved cartilage repair & delay cartilage degeneration in age mice while having a limited effect on bone healing, even a higher dosage. These results suggest that hBMP4 mRNA encapsulated with lipid nanoparticle represents a promising treatment for age-related OA.

Keywords: human BMP4 chemically modified mRNA; critical calvarial bone defect; osteoarthritis; age-related osteoarthritis; lipid nanoparticle; bone tissue engineering

1. Introduction

Age-related osteoarthritis (OA) affects tens of millions of patients, often causing disability, pain and affecting quality of life. Currently there is no disease modifying treatment. At the end stage of OA, patients often need joint replacement [1,2]. Segmental bone defects caused by trauma and tumor resection are challenging orthopaedic conditions to treat [3,4]. Autografts, allografts, and BMP2 protein therapy remain the current available clinical treatments. However, complications such as donor site morbidity, infection, and heterotopic bone formation have hindered their applications [5]. Hence, developing novel therapies to treat osteoarthritis or segmental defects is critically needed.

 doi:10.20944/preprints202604.0770.v1

Bone morphogenetic protein 4 (BMP4) plays diverse roles during development including promoting stem cell renewal [6,7] and enhancing induced pluripotent stem cell (iPSC) reprogramming efficiency [8–10]. BMP4 has also been shown to have anti-senescent, anti-steatotic, anti-inflammatory, and anti-fibrotic properties. In contrast, its antagonist Gremlin 1, which is particularly highly expressed in human visceral fat, is pro-senescent and antagonistic to BMP4 in non-alcoholic fatty liver disease [11]. Previously, it has been shown that muscle-derived stem cells (MDSC) retrovirally transduced to express human BMP4 improved cartilage repair in a rat model of MIA induced OA [12]. BMP4 promoted robust chondrogenic differentiation of human mesenchymal stem cells (MSCs), and coacervate-mediated delivery of various BMPs, including BMP4, promoted microfracture mediated cartilage repair in an osteochondral defect model [13]. BMP4 has also reversed age related declines in muscle derived stem cell proliferation and enhanced bone regeneration [14]. Therefore, BMP4 is a bone morphogenetic protein that can play multiple roles in bone and cartilage regeneration. Currently, BMP4 has not been used clinically for musculoskeletal tissues regeneration and repair due to concerns associated with gene therapy-based approaches.

Furthermore, mRNA encapsulated in lipid nanoparticles-mediated gene delivery has become increasingly feasible following the successful development of the COVID-19 mRNA vaccines to control the pandemic. BMP2 mRNA encapsulated in lipid nanoparticles has been shown to regenerate critical-sized long bone defects via endochondral bone formation, achieving outcomes equivalent to a clinical dose of BMP2 protein [15]. BMP9 mRNA complexed with nanoplex polyethylenimine (PEI) has also been shown to enhance calvarial bone defect repair and results in complete defect closure at a 50µg dose [16]. However, most studies have been performed on young animals, which have superior tissue regeneration compared to aged animals. Hence, the goal of this study was to investigate whether human BMP4 mRNA encapsulated with lipid nanoparticles will promote bone defect healing and cartilage repair in aged mice.

2. Materials and Methods

2.1. Human BMP4 (hBMP4) mRNA Preparation and Encapsulation

Human BMP4 clone was purchased from OriGENE (Cat#:SC108985) and subcloned for in vitro transcription. RNA was then purified and subsequently encapsulated in lipid nanoparticles according to a previous protocol [17], and its quality was verified using Tapestation.

2.2. Human BMP4 mRNA for Critical-Sized Calvarial Defect Healing Using Fibrin Sealant as Scaffold

This experiment was approved by Institutional Animal Care and Use Committee (IACUC #3817) of Colorado State University. Briefly, 18-month-old C57BL6J mice were divided into three groups (N=6-7, both males and females). Group 1: freezing medium (158µl) + fibrinogen (30µl) + thrombin (30µl) scaffold; Group 2: 25µg human BMP4 mRNA in 79µl + 79 µl mRNA freezing medium + Fibrinogen (30µl + thrombin (30µl) combined and applied to the defect; Group 3: 50µg mRNA in 158µl + Fibrinogen (30µl) + thrombin (30µl). The creation of a critical-size 5mm calvarial bone defect was performed as previously described [18]. Mouse skulls were shaved to remove fur. After sterilization with providine followed by 70% alcohol, an incision was made just off the midline of the scalp. The periosteum was removed, and a 5mm critical size defect was created with a 5mm diameter trephine drill. Human BMP4 mRNA mixed with thrombin was then added to the defect using a 200µl tip ring, and immediately 30µl of fibrin was added. Hold the tip ring for 1-2 minutes to allow for fibrin to form a fibrin-sealant hydrogel in the defect area. The tip ring was then removed and wounds were closed with sutures. Mice were recovered in a warm box and then transferred to their home cage.

 doi:10.20944/preprints202604.0770.v1

2.2.1. Live Micro-CT Scan to Monitor Bone Regeneration

Live micro-CT scanning was performed every two weeks as previously described [19] using viva-CT 80 (Scanco Medical LLC, Switzerland). The micro-CT scan parameters were 70kVP, 110μA and 30μm voxel size. All micro-CT analyses were performed using the built-in micro-CT software V7.1-2. For the overview analysis of new bone formation in the defect area, we used the 400×200 dimension to define the defect area using Gauss Sigma=0.8, Gauss support=1 and threshold 163. For new bone formation quantification, we quantified by carefully contouring the new bone manually and using the morph function of the software. The new bone was defined using Gauss Sigma=0.8, Gauss support=1 and threshold 163.

2.2.2. Bone Histology

Mice were sacrificed at 6 weeks after skull defect surgery after the last micro-CT scan. Skull tissue containing the defects were harvested, fixed in neutral buffered formalin (NBF) for 3 days, then decalcified with 10% EDTA plus 1% sodium hydroxide (PH=7.0) for 4 weeks. The skull tissues were cut at the front ¼ of the defect and the middle of the defect for tissue processing and embedding. The tissues were placed in cassettes and processed using a Tissue Processor (KD-TS3D1, KEEDE) and paraffin embedded using a tissue embedder (KD-BM-II, KEEDEE). Sections were then cut into 5μm thickness using Leica Microtome (Histocore MULTICUT, Leica System). Herovici's staining was performed using a protocol as previously described [19–21] to differentiate collagen type 1 (COL1) and type 3 (COL3). All reagents are from Sigma-Millipore. H&E staining was performed using Extra-Strength Hematoxylin and Eosin Y (alcoholic) from ANATECH LTD following the manufacturer's protocol. Histological images were captured with Nikon CIS microscope using NIS software.

2.3. Human BMP4 mRNA for the Treatment of Natural Aged Mice Osteoarthritis

2.3.1. Human BMP4 mRNA/LNP Intra-Articular Injection

This experiment was approved by IACUC of Colorado State University (Protocol#4839). 19-month-old C57BL6J mice including both males and females were divided into 3 groups: group 1 (CTL, N=8): intra-articular injection of mRNA freezing medium in 15.8μl; group 2 (N=7): intra-articular injection of 2.5μg lipid nanoparticle encapsulated hBMP4 mRNA (15.8 μl); group 3 (N=8): intra-articular injection of 5μg (15.8ul) lipid nanoparticle encapsulated hBMP4 mRNA. Intra-articular injections were performed in the left knee at baseline and repeated every three weeks for a total of 3 times. Mice were sacrificed 2 weeks after the last injection, and the knees were harvested and fixed in NBF.

2.3.2. Pain Measurement

Mechanical sensitivity (pain threshold) was measured using a Von Frey device at baseline and at 4 and 8 weeks post-injection as previously described [22]. Briefly, mice were placed in the metal mesh box individually and acclimated for 30 minutes. Von Frey Filaments were then applied to the plantar of the left paw. The filament was applied with enough force to elicit a withdrawal response. The stimulus intensity was recorded automatically by the device and documented immediately. This measurement was repeated 5 times for each mouse at 5-minute intervals, and the average of the 5 measurements was used to represent the pain threshold.

2.3.4. Micro-CT Scan and Analysis for Knee Joint

Mice were sacrificed at 8 weeks after IA injections of hBMP4 mRNA. The entire knee was scanned with Vivo-CT 80 using 70kvp, 110 μA and 15μm voxel size. The micro-CT was analyzed using built-in software and 3D images of the entire knee were reconstructed using Gauss Sigma=0.8, Gauss support =1, and threshold 163 to reveal heterotopic bone (HO) formation and general structural morphology of the knee as previous described [23].

 doi:10.20944/preprints202604.0770.v1

2.3.5. Histology

After the micro-CT scans, the tissues were decalcified with 10% EDTA plus 1% NaOH for 4 weeks, paraffin embedded and sectioned in 5μm thickness as stated in 2.2.2. Alcian blue staining was performed using IHC world protocol as previously described [24] to detect acid mucin and hyaluronic acid. Safranin O staining was performed using IHC world protocol with a slight modification to increase Safranin O step to 30 minutes to reveal the cartilage matrix glycosaminoglycans (GAG). Cartilage repair was evaluated using the Osteoarthritis Research Society International (OARSI) osteoarthritis histology score system [25] based on Safranin O and Alcian blue staining. Herovici's and H&E staining were also performed as described previously [26].

2.3.6. Immunohistochemistry Staining of COL2

Immunohistochemistry (IHC) staining of type 2 collagen (COL2) was performed to reveal cartilage specific matrix COL2. Briefly, paraffin sections were deparaffinized and rehydrated to deionized water. Slides were first subjected to antigen retrieval using 2% hyaluronidase in PBS for 30 minutes at room temperature (RT) as previously described [13]. Then, the slides were washed with PBS 3 times and blocked with 5% donkey serum in PBS for 1 hour at RT. Subsequently, the blocking solution was removed without washing, and 100μl mouse anti-COL2 antibody (#7048, 1:500 dilution, Chondrex Inc) diluted in blocking solution was applied and incubated at 4^{0}C overnight. On the second day, slides were washed with PBS 3 times for 5 minutes, and endogenous peroxidase was inactivated using 0.5% hydrogen peroxide in PBS for 10 minutes. Following another 3 washes with PBS, the slides were incubated with biotinylated horse anti-mouse secondary antibody (BA 2000, Vector Laboratories, Burlingame, CA, USA, 1:300 dilution) for 2 hours at room temperature. After three washes, slides were further incubated with ABC reagent (PK 6100, VECTASTAIN® Elite® ABC-HRP Kit, Peroxidase (Standard), Vector Laboratories) for 2 hours at room temperature. The slides were then washed 3 times with PBS and diaminobenzidine (DAB) color reaction kit (SK-4100, Vector Laboratories) was used to visualize the COL2-positive cells and matrix. Hematoxylin (H-3404, Vector laboratories) counterstaining was performed after the DAB color reaction. Immunohistochemistry images were captured using a NIKON-CI microscope.

2.3.6. Serum Cartilage Damage Marker Enzyme-Linked Immunosorbent Assay (ELISA)

Blood was collected at the time of sacrifice from the retro-orbital network and allowed to coagulate for 30 minutes. Serum was then isolated by centrifugation at 1500xg for 10 minutes and stored in a -80^{0}C freezer until analysis by ELISA. Hyaluronic acid (HA) levels were measured using a mouse Hyaluronic acid (HA) ELISA Kit (Cat#:EK730393,AFG Scientific) following the manufacturer's protocol. The standard curve was curve fit using a 4PL model, and serum concentration of HA was calculated from the 4PL curve using GraphPad Prism 10.2.

2.4. Statistical Analysis

All statistical analyses were performed using Graphpad Prism 10. Data was analyzed by ANOVA followed by Tukey's multiple comparisons test, or non-parameter tests if data was not normally distributed. $P<0.05$ was deemed statistically significant.

3. Results

3.1. HBMP4 mRNA In Vitro Transcription and Encapsulation Verification

A human BMP4 mRNA plasmid, purchased from Origene (Cat#:SC108985, NCBI Sequence ID: NM_110202, or NP_001193.1), was subcloned into a T7 promoter vector for in vitro transcription. In vitro transcription was performed by RNAcore from Houston Methodist Academic Institute. To generate chemically modified hBMP4 mRNA, in vitro transcription incorporated N1-methyl pseudo-urindine triphosphate (N1-M-pUTP) with CleanCap. The full size of transcribed hBMP4 mRNA is

 doi:10.20944/preprints202604.0770.v1

1603bp. After purification of hBMP4 mRNA, the quality was verified using Tapestation (Figure 1A). The hBMP4 mRNA was subsequently encapsulated with SM-102 lipid nanoparticles. The final hBMP4 mRNA/LNP quality met the quality requirement for particle size, polydispersity index (PDI), and Zeta potential (ZP) with a final concentration of 316µg/ml after encapsulation (Figure 1B,C).

A Tapestation image of hBMP4 mRNA before encapsulation

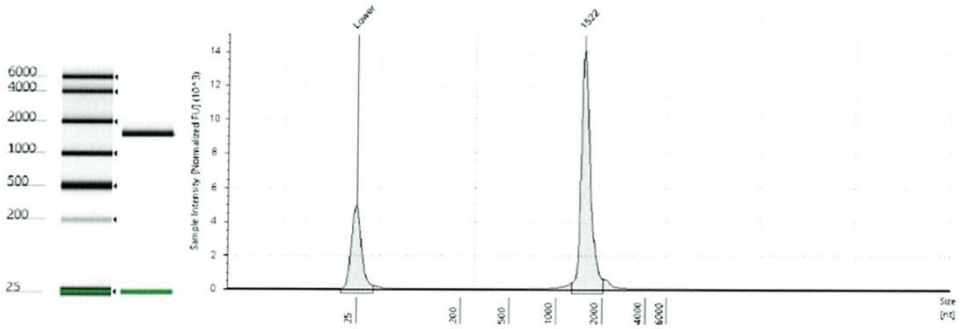

B Tapestation image of hBMP4 mRNA post LNP encapsulation

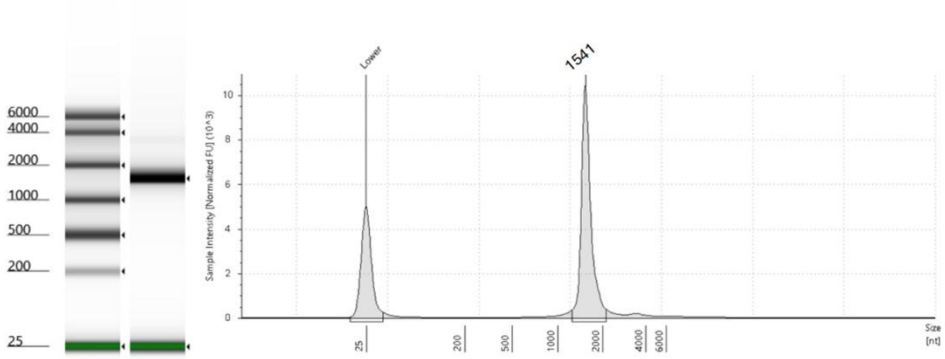

C

Parameter	Value
Size (nm)	93.47
PDI (a.u.)	0.24
ZP (mV)	-9.44
RNA Concentration (µg/ml)	316.84

Figure 1. hBMP4 mRNA in vitro transcription and encapsulation quality verification. (**A**) hBMP4 mRNA band size measured by Tapestation. (**B**) hBMP4 mRNA band size measured by Tapestation after LNP encapsulation. (**C**) hBMP4 mRNA/LNP particle size, PDI, Zeta potential, and hBMP4 RNA concentration measurements.

3.2. HBMP4 mRNA Promoted Limited Bone Regeneration in a Critical-Sized Calvarial Bone Defect in Aged Mice

Following application of hBMP4mNRA/LNP using a fibrin sealant scaffold immediately after creation of a critical-sized calvarial bone defect, we monitored the bone formation using live micro-CT scans at 2, 4 and 6 weeks post-surgery. A 3D Micro-CT overview of the entire defect and segmentalized new bone formation demonstrated minimal new bone formation at the edge of the critical-sized calvarial bone defect in the control group. Relatively more new bone formation was observed in the 25µg and 50µg hBMP4 mRNA groups at all time points. However, a complete defect healing was not observed, in any groups, by 6 weeks (Figure 2A). Quantification of new bone

 doi:10.20944/preprints202604.0770.v1

formation in the defect area revealed significantly higher new bone volumes in the 25µg and 50µg groups at 2 weeks after the application of hBMP4 mRNA, but no significant differences were found at 4 and 6 weeks after application compared to control group (Figure 2B).

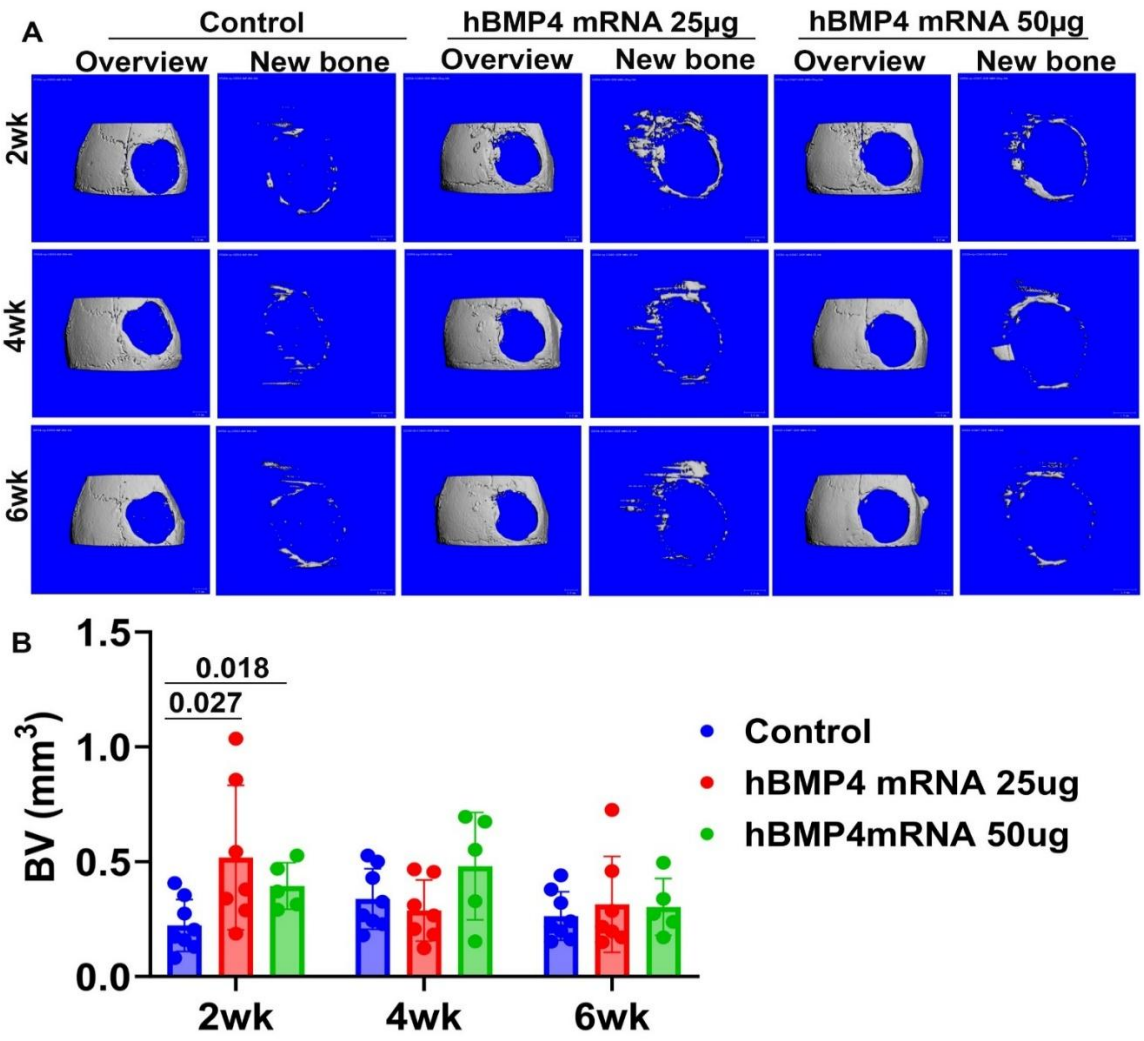

Figure 2. Micro-CT Live scan 3D images to monitor bone defect healing after implantation of hBMP4 mRNA (**A**) Micro-CT 3D overview of the entire defect and segmentalized new bone formation at each 2, 4, and 6 weeks in different groups: minimal new bone formation was detected at the edge of the critical size calvarial bone defect. Relatively more new bone formation in 25µg and 50µg hBMP4 mRNA groups was observed at all time points. However, a complete defect healing was not observed, in any groups, by 6 weeks. (**B**) Quantification of new bone formation in the defect area: new bone volumes are significantly higher in 25µg and 50µg group at 2 weeks after application of hBMP4 mRNA, but no significant differences were found at 4 and 6 weeks after application. Exact P values are indicated between group bars.

3.3. Histology Revealed Minimal New Bone Formation Mediated by hBMP4 mRNA/LNP in Critical-Sized Calvarial Bone Defect When Delivered with Fibrin Sealant

We performed Herovici's staining to detect COL1 (a major bone matrix) and COL3, a fibrotic collagen. At 20X, the entire defect view was revealed at ¼ of the defect (edge) or middle of the defect. The residual host bone is evident on both edges of the defect for all groups with intense pink-red staining. The CTL group showed no bone formation in either edge or in the middle of the defect. In the 25µg group, some new, island-like, bone was detected at the edge of the defect. No pink stained COL1 was detected in the middle of the defect. In the HBMP4 50µg group, no pink-red COL1 was detected in either edge or the middle of the defect. At 100X, in the CTL group, only blue stained COL3

 doi:10.20944/preprints202604.0770.v1

was detected in either edge or the middle of the defect. Pink-stained COL1 was detected in the edges of the defect of the HBMP4 mRNA 25μg group (black arrows), but not in the middle of the defect. No pink-stained COL1 was detected in the edge and middle of the defect in the hBMP4 mRNA 50μg group (Figure 3A). H&E staining revealed dense trabecular residual host bone. The defect was filled with fibrotic tissue in the CTL group. There was also no new bone formation in the hBMP4 25μg group at the edges or the middle of the defect. At the edge region, a small bone island of dense tissue was detected (blue arrows), and only fibrotic tissue in the middle of the defect was found in the 50μg hBMP4 mRNA/LNP group. The new bone did not have trabecular bone structure (Figure 3B).

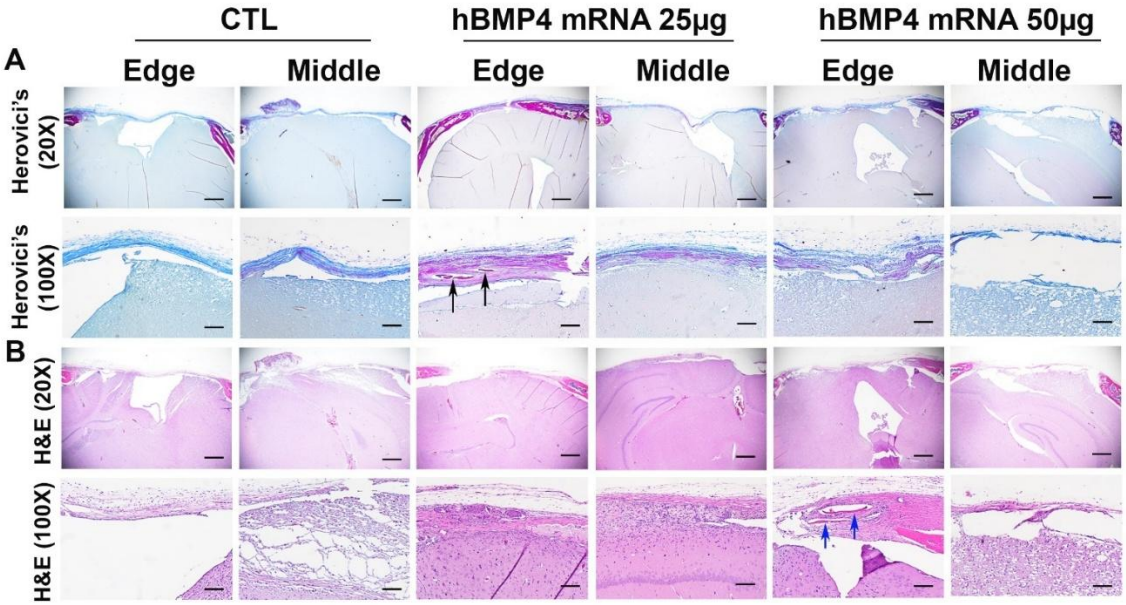

Figure 3. Histology of the skull defect after hBMP4 mRNA application. (**A**) Herovici's staining to reveal new bone formation: COL1 stained in pink-red while COL3 stained in dark blue. No new bone formation was revealed in the defect area in CTL group in both edge and middle of the defect. Only blue stained COL3 $^{+}$scar tissue was observed. In the 25μg group, only island bone was detected at the edge of the defect (black arrows). No new bone was detected in the middle of the defect. No new bone formation in the defect area was found at this section level for the 50μg hBMP4 mRNA group. (**B**) H&E staining. No new pink-stained new bone was detected in the edge and middle of the defect area for CTL and 25μg hBMP4 RNA group. Only island bone was detected at the edge of the defect of 50μg hBMP4 mRNA group as indicated by blue arrows. Scale bars = 500μm for 20X and 100μm for 100X.

3.4. Micro-CT Results Revealed No Increase in Heterotopic Bone Formation in the Knee Joint at 8 weeks After Intra-Articular Injection of BMP4 mRNA

3D Micro-CT images revealed a mild heterotopic ossification (HO) formation (red arrows) in each group, which was likely caused by mild injury due to injection or age-related osteophyte formation. HBMP4 mRNA at 2.5 and 5μg doses did not increase rate of HO formation. The large HO formation in one sample from the hBMP4 mRNA 5μg group was likely due to leakage of injected hBMP4 mRNA into the muscle (Figure 4A).

 doi:10.20944/preprints202604.0770.v1

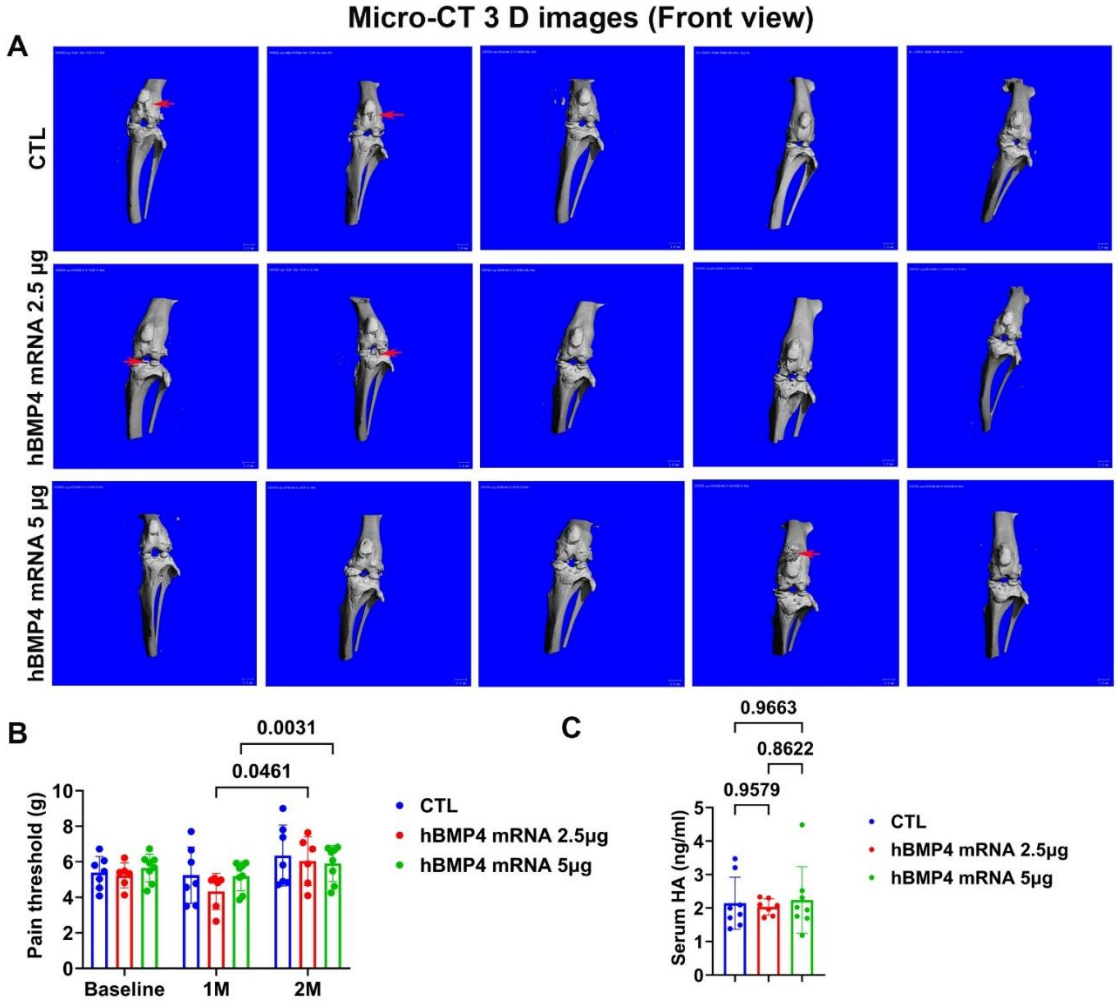

Figure 4. Micro-CT results of knee joint at 8 weeks after BMP4 mRNA injection. (**A**) Micro-CT 3D images of the knee. No increase in heterotopic bone formation was observed in BMP4 mRNA at 2.5µg and 5µg doses compared to CTL group. Red arrows point to HO formation. Scale bars = 1mm. (**B**) Von Frey pain threshold. There was no statistical differences at baseline and 1M after mRNA injection. At 2M, both BMP4 mRNA 2.5 and 5µg had increased pain thresholds compared to 1M after injection which indicated reduced pain. Exact P values are indicated between group bars. (**C**) ELISA results of serum HA. Exact P values are indicated between group bars.

3.5. hBMP4 mRNA Intra-Articular Injection Appeared to Alleviate Pain Threshold Measured by Von-Frey Device

We also measured pain using a Von-Frey device before injection and again at 1 and 2 months after injection. The pain threshold was assessed using a Von Frey device, which measures the paw withdrawal response threshold to the applied force using sharp filaments. A higher threshold of applied force before paw withdrawal means less sensitivtiy to pain. Our results revealed no significant difference between groups at baseline, but pain threshold increased from 1 month to 2 months after injection in the 2.5 and 5µg hBMP4 mRNA groups after IA injection (Figure 4B). These results indicated IA injection of hBMP4 mRNA/LNP may alleviate pain of aged-related natural osteoarthritis.

3.6. Intra-Articular Injection of hBMP4 mRNA Did not Significantly Change Serum Cartilage Damage Marker Hyaluronic Acid (HA)

We further performed an ELISA analysis of serum hyaluronic acid (HA). We found no significant differences among different groups (Figure 4C).

 doi:10.20944/preprints202604.0770.v1

3.7. hBMP4mRNA/LNP Intra-Articular Injection Prevented Age-related Cartilage Loss and Improved Histology Score

To evaluate whether hBMP4 mRNA/LNP can improve age-related osteoarthritis, Safranin O staining was performed. The best and worst cartilage OA repair was shown for all groups. The entire medial side of the knee joint structure is displayed with the femur on the left side and the tibia on the right side (Figure 5A). The CTL group had 3 mice with severe cartilage damage and the mouse with the worst repair had no orange-red-stained cartilage in the articular cartilage surface (denuding) as demonstrated in both the femoral condyle and tibial plateau cartilage (Figure 5B,C). Both 2.5 and 5µg hBMP4 mRNA groups had only 1 mouse with severe cartilage damage with partial cartilage loss and complete loss of the orange red matrix. Other mice from each group demonstrated relatively mild or even normal cartilage morphology (Figure 5A–C). Alcian blue staining labeled cartilage matrix acid mucins and hyaluronic acid in blue, revealing a complete loss of blue-stained matrix in the worst repaired joint of the CTL group. In contrast, hBMP4 mRNA/LNP injected mice had only partial cartilage loss in the worst case (Figure 5D–F). Furthermore, OARSI histology score of medial femoral condyle was significantly lower (better repair) in the two hBMP4 mRNA groups when compared to the CTL group, but there were no differences between the two hBMP4 mRNA groups (Figure 5G). OARSI histology score of medial tibial plateau cartilage was also significantly lower in the two hBMP4 mRNA dosage groups compared to the CTL group with no difference between the two hBMP4 mRNA groups (Figure 5H)

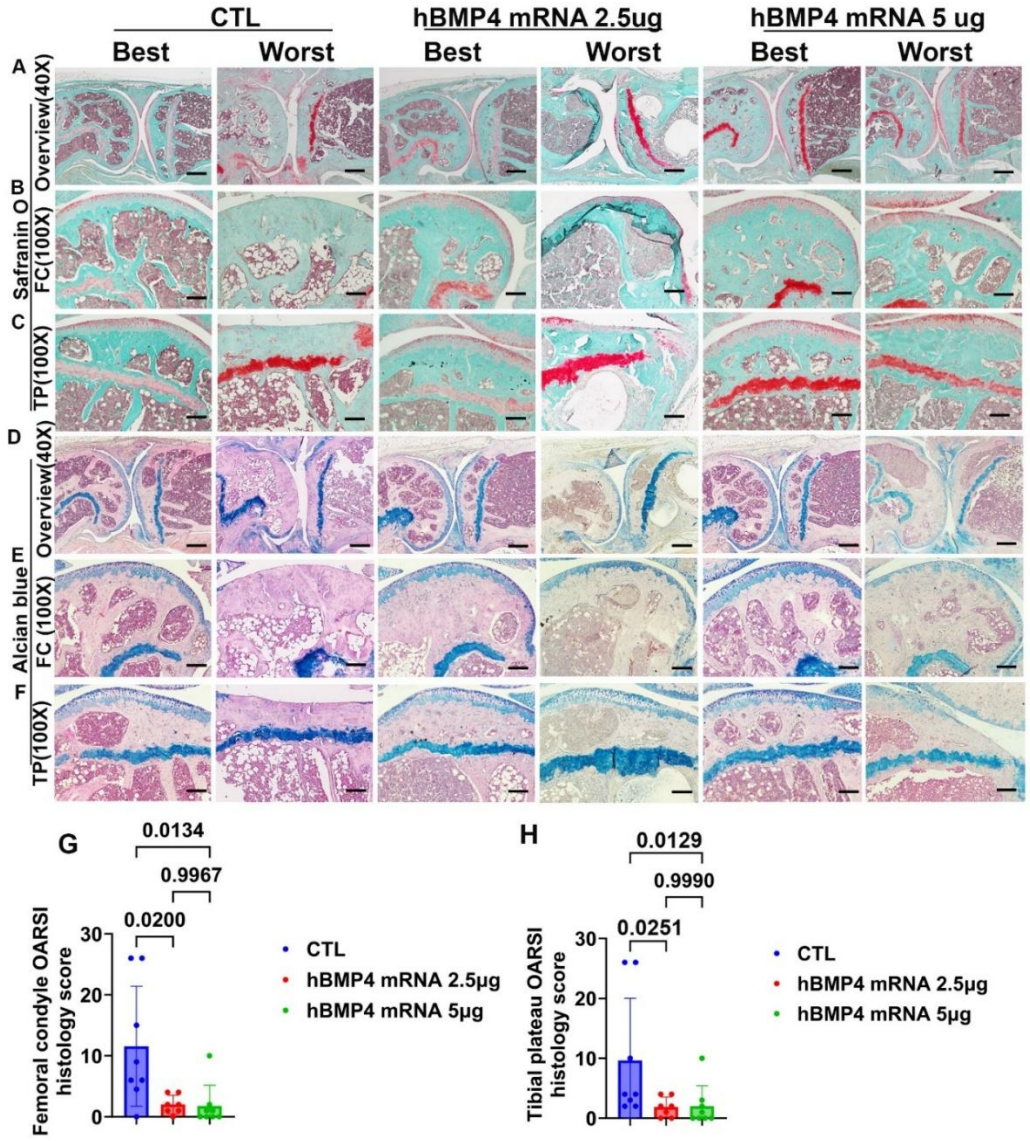

 doi:10.20944/preprints202604.0770.v1

Figure 5. Aged cartilage histology after IA injection of hBMP4 mRNA/LNP. (**A–C**) Safranin O staining of entire knee joints (40X), femoral condyle and tibial plateau cartilage. Best and worst knee repair are shown for all groups. Cartilage or chondrocytes GAG stained orange-red, nuclei stained black and cytoplasm stained green. (**D–E**) Alcian blue staining of entire knee, femoral condyle and tibial plateau. Acid mucin and HA stained blue. Nuclei are stained red and cytoplasm is stained pale pink. (**G**) Femoral condyle OARSI histology score. (**H**) Tibial plateau histology score. Scale bars= 250μm for 40X and 100μm for 100X. Exact P values are indicated between group bars.

3.8. hBMP4mRNA/LNP Intra-Articular Injection Maintained Cartilage Matrix During Aging

We performed immunohistochemistry for cartilage specific matrix COL2. COL2 was stained brown both inside chondrocytes and in the extracellular matrix of the cartilage. COL2 was completely lost in the CTL group's worst-repair, while there was only partial loss in the worst repair of the two hBMP4 mRNA dosage groups. Focal COL2 positive cells were detected in the proliferation zone of the two hBMP4 mRNA groups (Figure 6A–C). Herovici's staining revealed mixed blue and red staining in the best cartilage repair animal of each group, while only pink COL1 was present in the worst repair of the CTL group, and the two hBMP4 mRNA groups showed partial cartilage loss (Figure 6D,E). H&E staining revealed typical morphology in the animal with the best cartilage repair and only subchondral bone in the worst repair of the CTL group. In contrast, there was only loss of partial cartilage cells in the worst repair of the two hBMP4 mRNA groups (Figure 6G,H).

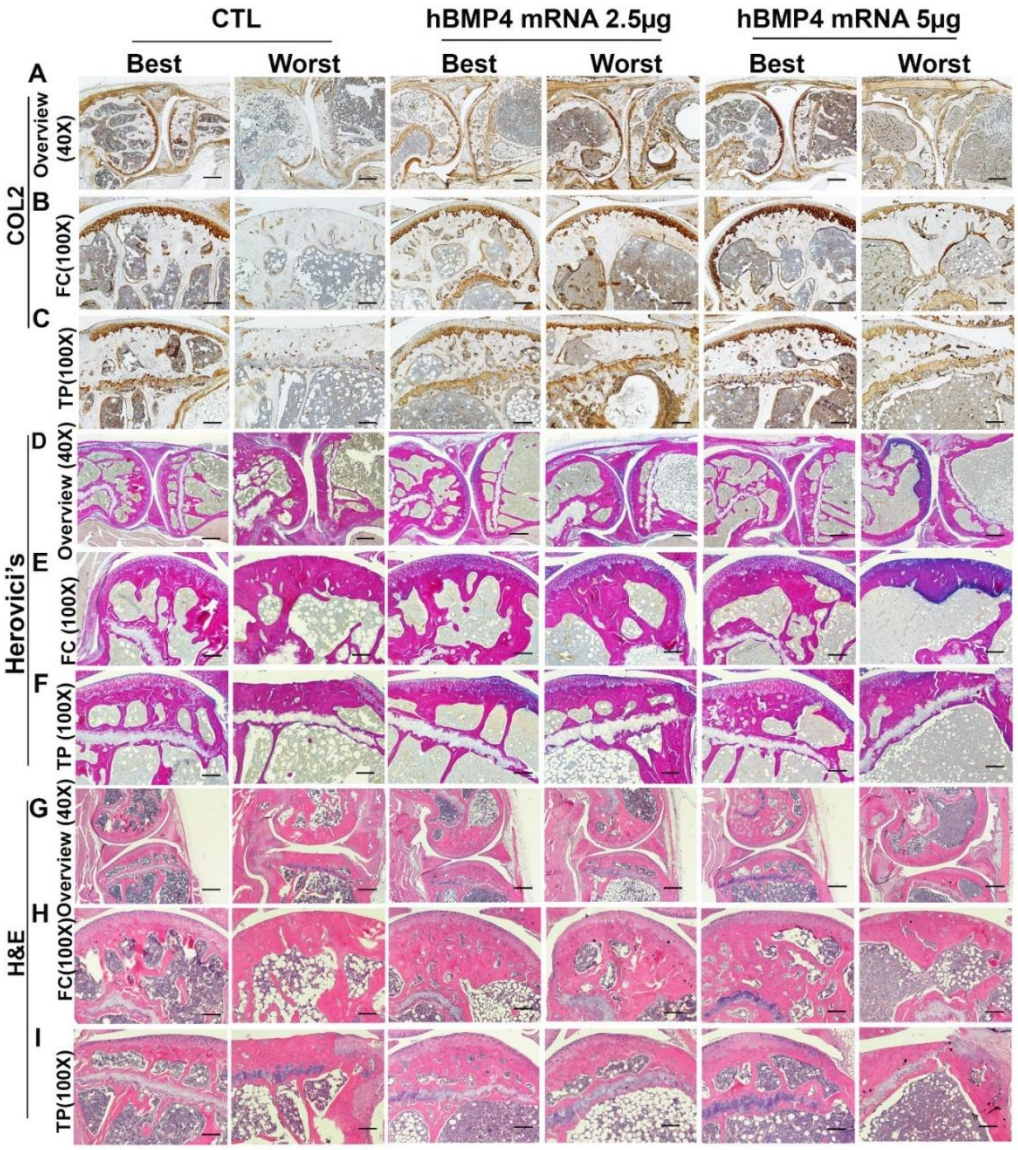

 doi:10.20944/preprints202604.0770.v1

Figure 6. COL2 IHC, Herovici's staining, and H&E staining at 8 weeks after IA hBMP4 mRNA injection. (**A–C**) Immunohistochemistry of COL2 for entire knee, femoral condyle and tibial plateau. COL2 stained brown in chondrocytes and cartilage matrix as well as residual expression in subchondral bone. (**D–F**) Herovici's staining for entire knee, femoral condyle and tibial plateau. COL1 stained in pink-red while COL3 stained in dark blue. (**G–I**) H&E staining to reveal general morphology of articular cartilage. Nuclei stained blue and cytoplasm stained red. Scale bars = 250μm for 40X and 100μm for 100X.

4. Discussion

In this study, we found that hBMP4 mRNA/LNP at 25μg and 50μg dosages only promoted relatively more bone formation than control, at earlier time points after the creation of a bone defect when delivered using fibrin sealant hydrogel. The new bone formation did not further increase compared to control at later time points as revealed by micro-CT and histology. However, IA injection of hBMP4 mRNA/LNP at 2.5μg and 5μg doses into the knees of aged mice improved cartilage repair by decreasing the OARSI histology score of articular cartilage of both the femoral condyle and tibial plateau as demonstrated by Safranin O and Alcian blue staining, as well as immunohistochemistry staining of collagen type 2 (COL2). The hBMP4 mRNA injection did not increase HO formation in the knee compared to the CTL injection group.

BMPs are a group of the most potent bone growth factors for bone tissue engineering [18] and have been approved by FDA for several clinical applications [27]. Following the successful use of the COVID-19 mRNA vaccine to control the COVID-19 pandemic, several studies have reported the use of mRNA/LNP as a delivery approach to generate therapeutic proteins in the host cells to promote bone regeneration. Elangovan S et al. first demonstrated that chemically modified ribonucleic acid (cmRNA) encoding BMP-2 delivered using polyethylenimine (PEI) increased in BMP-2 protein expression in transfected human bone marrow mesenchymal stem cells (hBMMSCs) compared to PEI-BMP2 pDNA transfected hBMMSCs at the same dose. When implanted into rat calvarial bone defect, the PEI-cmRNA encoding BMP-2 (25μg BMP-2 cmRNA) polyplexes regenerated more bone in the defect with higher bone volume (BV/TV) compared to 25μg BMP-2 pDNA polyplexes and significantly higher BV/TV than empty defect group. Histological results showed more mature mineralized bone tissue in the BMP-2 PEI-cmRNA group compared to minimal new bone formation in the edge of the defect in the pDNA group [28]. Surisaeng T et al. showed that BMP-2 cmRNA/LNP loaded on either silk fibroin (SF) or gelatin silk fibroin (G) scaffolds both increased the amount of mineralized bone matrix in the defect and percentages of calvarial defect closure, as well as BV/TV compared to empty defects. When using the G scaffold, all BMP-2 mRNA doses (1.5, 5, and 15μg) significantly increased BV/TV, while using the SF scaffold, only the 15μg dose of BMP-2 mRNA showed a statistically significant increase in BV/TV indicating G scaffold is more suitable for delivery of BMP2 cmRNA. However, only less than 60% defect closure were observed in either scaffold group [29]. Furthermore, Khorsand B et al. also compared the bone regeneration potential of nanoplexes of polyethylenimine (PEI)-delivered BMP-9 cmRNA (10μg) and BMP-9 pDNA (10μg) loaded into perforated collagen membranes (PCMs) using a critical-sized calvarial defect model in rats. It was found that PEI delivered-cmRNA encoding BMP-9 loaded on PCMs significantly enhanced new bone formation and BV/TV compared to the scaffold only group, and a non-significant increase in BV/TV compared to PEI-pDNA-PCM group [16]. The same group of authors also compared cmRNA encoding BMP-2 and BMP-9 complexed with PEI at a 50μg dose. When loaded on collagen scaffolds, freeze dried, and implanted into the 5 mm calvarial bone defect in rats, both BMP-2 and BMP-9 cmRNAs regenerated significantly more bone compared to the empty defect (control) group with complete defect closure, while control group largely had no bone formation [30].

BMP2 mRNA has also been investigated for long bone defect healing. Balamayor E et al. reported that BMP-2 cmRNA transfected stem cells demonstrated enhanced osteogenic differentiation in vitro. When BMP-2 cmRNA (2.5μg) loaded on Fibrin + C12-EPE/hBMP-2 cmRNA lipoids which subsequently implanted into a 3 mm non-critical sized rat femoral defect model, more mineralized callus bone was formed at 2 weeks compared to the fibrin only control defect. At later

 doi:10.20944/preprints202604.0770.v1

time points, more mature bone was observed in the BMP-2 cmRNA group as revealed by histology [31]. Furthermore, Badieyan ZS et al., developed vacuum-dried cmRNA-loaded collagen sponges, termed transcript activated matrices (TAMs). BMP-2 cmRNA at 2.5μg loaded on TAM applied to a 2 mm drill hole non-critical rat femur defect significantly increased bone callus volume, bone area, and osteoid volume as confirmed by μCT and histomorphometric analysis [32]. De La Vega RE et al. compared bone regeneration of BMP-2 cmRNA with recombinant BMP-2 protein (rhBMP-2) in a rat critical sized femoral defect model. Different doses (12.5ug to 50ug) of BMP-2 cmRNA or rhBMP-2 protein were loaded on a collagen sponge and implanted into a 5mm femur defect covered with a deep muscle pouch. It was found that BMP-2 cmRNA promoted bone repair in a dose-dependent manner, with complete defect bridging found at 50μg but not at lower doses. The 50μg cmRNA group also showed greater BV/TV and Tb.N at 8 weeks after surgery, indicating faster mechanical recovery and bone remodeling than control group, and produced superior bone quality when compared with all other groups. Similar results were observed with the application of 11μg rhBMP-2 [15].

Previously, we have demonstrated that retro-BMP4GFP transduced murine MDSCs efficiently regenerated bone in calvarial bone defect and completely healed bone defects in 4 weeks when MDSCs secreted about 19ng/million cells/24 hours [33]. We also demonstrated that BMP4 can improve the osteogenic potential of aged MDSCs and promote bone formation of aged MDSCs via regulating cell cycle inhibitors such as P16 [14], but no study has been conducted using human BMP4 mRNA for calvarial bone defect repair. Therefore, we chose chemically modified BMP4 mRNA for this study. However, even high dose of hBMP4 mRNA (50μg/5mm defect) did not significantly promote bone defect healing in aged mice, in the current study. This contrasts with what we have done using coacervate sustain-release biomaterials with rhBMP4 protein. Only 2μg of rhBMP4 protein can generate more bone than 50μg of mRNA using the same fibrin sealant scaffold [18] and is negligible compared to BMP4 transduced MDSCs which generated more than 100 mm^3 of new bone using a fibrin sealant scaffold with complete healing in 4 weeks [33]. The reason for the inefficiency of hBMP4 mRNA/LNP might be that we used fibrin sealant hydrogel as scaffold which is hydrophilic while the LNP is hydrophobic. The other reason might be that we applied the BMP4 mRNA immediately after the defect creation, meaning there are very few cells present for BMP4 mRNA to transfect to express target proteins. The third reason might be that most reported chemically modified mRNA can only express target proteins within 1 week of administration. Therefore, it might be more effective when applied at 1 week after injury when host repairing cells such as MSCs have already migrated to the defect area. Previous studies using cmBMP2 mRNA also resulted in only partial defect closure in a cavarial bone defect model when using doses of 25μg or less [16,28,29]. Only 50μg cmBMP2 or BMP9 mRNA/PEI loaded on collagen scaffolds results in complete defect closure [30]. Therefore, a scaffold that maintains BMP cmRNA in the defect until cells have migrated into the defect is also important. Overall, cmRNA required a much higher dose to achieve regenerative effects similar to those of proteins as demonstrated by other researchers and by us.

Several studies have also investigated cmRNA for cartilage repair. In 2016, Aini L et al. developed two polyethylene glycol (PEG)-polyamino acid block copolymer-based polyplex nanomicelles called PEG-PAsp(DET) and PEG-PAsp(TET) to deliver Runt related transcription factor 1 (Runx1P) cmRNA. Intra-articular injection of Runx1 mRNA (1μg in 20μl volume every 3 days for one month) via PAsp(DET) nanomicelles insignificantly improved medial collateral ligament (MCL)- and medial meniscus (MM)-transection-induced OA, compared to GFP mRNA. In contrast, delivery same dose of Runx1 mRNA using PEG-PAsp(TET) nanomicelles in the same OA model induced Runx1 expression in both superficial and middle zones of the articular cartilage, significantly decreased OARSI histology score and inhibited osteophytes formation, and upregulated SOX9 and COL2 expression and cell proliferation in the cartilage [34]. Furthermore, Pezzotti G et al. used Raman spectroscopic analysis and demonstrated the mechanism of cartilage restoration was attributed to activation of remaining chondrocytes by Runx1 cmRNA that resulted in increased hyaluronic acid synthesis and restoration of organized collagen secondary structures [35]. Additional study

 doi:10.20944/preprints202604.0770.v1

demonstrated that intra-articular injection of IGF-1 mRNA transfected adipose derived stem cells (ADSCs) (2×10^5) at 1 and 2 weeks post-DMM surgery ameliorated articular cartilage degeneration as revealed by decreased OARSI histology score and increased COL2 and ACAN expression [36].

Several studies also used fibroblast growth factor 18 (FGF-18) mRNA for cartilage repair. Huang K et al. developed a new lipid nanoparticle TG6A with branched tails and five ester bonds with higher efficiency of delivery compared to commercialized DLin-MC3-DMA and ALC-0315 lipid nanoparticles. MSCs transfected with TG6A LNP-encapsulated circular FGF-18 mRNA enhanced chondrogenic differentiation in an in vitro 3D pellet culture model. Circular FGF18 cmRNA-engineered MSCs improved cartilage repair in a rat OA model, as revealed by thicker cartilage layers, reduced histopathological scores, maintenance of zone structure, and higher type II collagen and extracellular matrix (ECM) deposition compared to untreated control [37]. Sun M et al. designed a novel articular cavity-localized lipid nanoparticle (LNP) named WG-PL14 that could increase in mRNA expressionapproximately 30-fold and enriched in articular cavity compared to commercial MC3 lipids after intra-articular injection. Intra-articular injection of 2μg (in 20μl/knee, once a week for 3 weeks) cmRNA encoding rhFGF-18 complexed with WG-PL14 LNPs delayed OA progression in a ACLT induced OA model as demonstrated by increased cartilage extracellular matrix (ECM)-related genes such as COL2 and ACAN, and decreased COL1, MMP13 and IL1β. FGF18 cmRNA also decrease osteophytes formation and increased tibial subchondral bone BV/TV,Tb.Th, bone mineral density and improved pain response [38]. Kong K et al. also showed that LNP/FGF18 mRNA can penetrate deeper into cartilage layers than proteins. Intra-articular injection of FGF18 mRNA/LNP (6μg weekly in 20μl) or 500 ng FGF18 protein (in 20μl) for 8 weeks in the joint of DMM-induced and age-related OA models improved OA phenotype through activation of the FOX3A-autophage pathway, decreased degeneration and senescence [39]. cmRNA has also been used for osteochondral defect repair. Fontana G et al. used mineral coated microparticles (MCM) and fluoride MCM (FMCM) to deliver transforming growth factor 1 (TGFβ-1) cmRNA. After loaded TGFβ-1 mRNA on FMCMs, they transfected bone marrow aspirate (BMAC) and then combined with autologous peripheral blood to form a clot, which was implanted into a 2.7mm condyle osteochondral defect created in a rabbit knee. BMAC-TGFβ-1 mRNA regenerated cartilage with increased type II collagen and glycosaminoglycan deposition, as well as reduced COL1 formation but did not significantly improve Odriscoll's histology scores [40].

In our study, we found injection of 2.5μg and 5μg cmBMP4 mRNA every 3 weeks for a total of 3 administrations prevented age-related cartilage loss and did not increase HO formation in the knee joints of aged mice. This contrasts with the need for a higher dose of cmhBMP4 mRNA for bone repair, likely because the knee joint contains cells that the injected mRNA can transfect and subsequently produce BMP4 protein to exert effects. Previous studies demonstrated that intra-articular injection of a lower dose of Runx1 mRNA (1μg in 20μl volume every 3 days for one month using PEG-PAsp(TET) rather than PEG-PAsp(DET) promoted repair of OA induced by MCL and MM transection [34]. Using a novel articular cavity-localized lipid nanoparticle (LNP) named WG-PL14 to deliver a low dose of FGF18 mRNA by intra-articular injection (2μg in 20μl/knee, once a week for 3 weeks) ameliorated ACLT induced OA progression [38]. More recently, Kong K et al. reported intra-articular injection of FGF18 mRNA/LNP (6μg in 20ul weekly) or FGF18 protein (500ng in 20μl weekly) for 8 weeks in the joint of DMM-induced and age-related OA models improved OA symptoms via activation of the FOX3A-autophage pathway, protecting chondrocytes from degeneration and senescence. It is noticeable that FGF-18 protein administered at a much lower dose achieved similar therapeutic effect to those of a much higher dose of FGF-18 mRNA [39]. These studies, together with our study, indicate smaller doses of cmRNA are required for cartilage repair and regeneration when compared to the higher dose needed for bone repair. Further, using BMPs to treat cartilage damage, especially osteochondral defects, may be more effective because BMPs not only promote cartilage repair, but also promote subchondral bone defect healing as we previously demonstrated using coacervate biomaterials to sustain release BMPs [13]. Therefore, cmRNA is more promising for cartilage repair.

 doi:10.20944/preprints202604.0770.v1

5. Conclusions

In summary, we found Human BMP4 mRNA delivered with lipid nanoparticles promoted limited new bone formation and defect repair in critical-sized calvarial bone defects in aged mice. In contrast, an intra-articular injection of a lower dose of BMP4 mRNA (ten times lower) improved cartilage repair and prevented cartilage loss in aged-related OA. Therefore, hBMP4 mRNA may represent a novel therapy for treatment of age-related OA.

Author Contributions: Conceptualization: X.G. and J.H.; methodology, X.G., Z.X., M.H., K.N., A.C., L.H. L, C.M.; formal analysis, X.G.; investigation, X.G., Z.X.,M.H., K.N., A.C, L.H. L, C.M.; resources, J.H.; data curation, X.G.; writing-original draft preparation; X.G.; writing-review and editing, J.H.,B.F., J.P.C,F.T.,M.J.P.; visualization, X.G.; supervision, X.G.,J.H.; project administration, J.H.,M.J.P.; funding acquisition, J.H. All authors have read and agreed to the final version of the manuscript.

Funding: This project is supported by Philanthropy gifts from the Musculoskeletal Regeneration Partnership Fund by Mary Sue and Michael Shannon and the Donna Giordano Family.

Data availability statement: Original data will be available from corresponding authors upon request.

Acknowledgments: We thank Laura Chubb from Dr. Ehrhart's lab for providing support to animal protocol, and providing the surgical suite, and surgery setup.

Conflicts of Interest: All authors declared no conflict of interest.

References

1. Hunter, D. J.; Bierma-Zeinstra, S., Osteoarthritis. *Lancet* **2019,** 393, (10182), 1745-1759.
2. Rashidi, A.; Bastan, M. M.; Golestani, A.; Azadnajafabad, S.; Rezaei, N.; Zeinodinimeymand, M.; Busehail, M.; Yaqoob, M.; Heidari-Foroozan, M.; Rashidi, M. M., Burden of osteoarthritis in North Africa and Middle East from 1990 to 2021: findings from the Global Burden of Disease 2021 study. *Clin Rheumatol* **2025**.
3. Kempny, T.; Holoubek, J.; Polovko, J.; Sedivy, O.; Votruba, T.; Kachlik, D.; Pilny, J., Reconstruction of large post-traumatic segmental femoral defects using vascularised bone flaps: a retrospective case series. *BMC Musculoskelet Disord* **2024,** 25, (1), 919.
4. Tsang, S. J.; van Rensburg, A. J.; van Heerden, J.; Epstein, G. Z.; Venter, R.; Ferreira, N., The management of critical bone defects: outcomes of a systematic approach. *Eur J Orthop Surg Traumatol* **2024,** 34, (6), 3225-3231.
5. Shen, J.; Wei, Z.; Wu, H.; Wang, X.; Wang, S.; Wang, G.; Luo, F.; Xie, Z., The induced membrane technique for the management of infected segmental bone defects. *Bone Joint J* **2024,** 106-B, (6), 613-622.
6. Ying, Q. L.; Nichols, J.; Chambers, I.; Smith, A., BMP induction of Id proteins suppresses differentiation and sustains embryonic stem cell self-renewal in collaboration with STAT3. *Cell* **2003,** 115, (3), 281-92.
7. Kirilly, D.; Spana, E. P.; Perrimon, N.; Padgett, R. W.; Xie, T., BMP signaling is required for controlling somatic stem cell self-renewal in the Drosophila ovary. *Dev Cell* **2005,** 9, (5), 651-62.
8. Samavarchi-Tehrani, P.; Golipour, A.; David, L.; Sung, H. K.; Beyer, T. A.; Datti, A.; Woltjen, K.; Nagy, A.; Wrana, J. L., Functional genomics reveals a BMP-driven mesenchymal-to-epithelial transition in the initiation of somatic cell reprogramming. *Cell Stem Cell* **2010,** 7, (1), 64-77.
9. Chen, J.; Liu, J.; Yang, J.; Chen, Y.; Chen, J.; Ni, S.; Song, H.; Zeng, L.; Ding, K.; Pei, D., BMPs functionally replace Klf4 and support efficient reprogramming of mouse fibroblasts by Oct4 alone. *Cell Res* **2011,** 21, (1), 205-12.
10. Hayashi, Y.; Hsiao, E. C.; Sami, S.; Lancero, M.; Schlieve, C. R.; Nguyen, T.; Yano, K.; Nagahashi, A.; Ikeya, M.; Matsumoto, Y.; Nishimura, K.; Fukuda, A.; Hisatake, K.; Tomoda, K.; Asaka, I.; Toguchida, J.; Conklin, B. R.; Yamanaka, S., BMP-SMAD-ID promotes reprogramming to pluripotency by inhibiting p16/INK4A-dependent senescence. *Proc Natl Acad Sci U S A* **2016,** 113, (46), 13057-13062.
11. Baboota, R. K.; Rawshani, A.; Bonnet, L.; Li, X.; Yang, H.; Mardinoglu, A.; Tchkonia, T.; Kirkland, J. L.; Hoffmann, A.; Dietrich, A.; Boucher, J.; Bluher, M.; Smith, U., BMP4 and Gremlin 1 regulate hepatic cell senescence during clinical progression of NAFLD/NASH. *Nat Metab* **2022,** 4, (8), 1007-1021.

 doi:10.20944/preprints202604.0770.v1

12. Matsumoto, T.; Cooper, G. M.; Gharaibeh, B.; Meszaros, L. B.; Li, G.; Usas, A.; Fu, F. H.; Huard, J., Cartilage repair in a rat model of osteoarthritis through intraarticular transplantation of muscle-derived stem cells expressing bone morphogenetic protein 4 and soluble Flt-1. *Arthritis Rheum* **2009,** 60, (5), 1390-405.
13. Gao, X.; Wright, N.; Huard, M.; Tan, J.; Ruzbarsky, J.; Lu, A.; Chubb, L.; Tuan, R.; Philippon, M. J.; Wang, Y.; Huard, J., Comparison of 5 BMPs for their chondrogenic potentials and microfracture-mediated cartilage repair using heparin/PEAD coacervate sustained release polymer. *Bioact Mater* **2025,** 52, 588-603.
14. Cheng, H.; Gao, X.; Huard, M.; Lu, A.; Ruzbarsky, J. J.; Amra, S.; Wang, B.; Huard, J., Bone morphogenetic protein 4 rescues the bone regenerative potential of old muscle-derived stem cells via regulation of cell cycle inhibitors. *Stem Cell Res Ther* **2022,** 13, (1), 385.
15. De La Vega, R. E.; van Griensven, M.; Zhang, W.; Coenen, M. J.; Nagelli, C. V.; Panos, J. A.; Peniche Silva, C. J.; Geiger, J.; Plank, C.; Evans, C. H.; Balmayor, E. R., Efficient healing of large osseous segmental defects using optimized chemically modified messenger RNA encoding BMP-2. *Sci Adv* **2022,** 8, (7), eabl6242.
16. Khorsand, B.; Elangovan, S.; Hong, L.; Kormann, M. S. D.; Salem, A. K., A bioactive collagen membrane that enhances bone regeneration. *J Biomed Mater Res B Appl Biomater* **2019,** 107, (6), 1824-1832.
17. Nelson, A. L.; Mancino, C.; Gao, X.; Choe, J. A.; Chubb, L.; Williams, K.; Czachor, M.; Marcucio, R.; Taraballi, F.; Cooke, J. P.; Huard, J.; Bahney, C.; Ehrhart, N., beta-catenin mRNA encapsulated in SM-102 lipid nanoparticles enhances bone formation in a murine tibia fracture repair model. *Bioact Mater* **2024,** 39, 273-286.
18. Gao, X.; Hwang, M. P.; Wright, N.; Lu, A.; Ruzbarsky, J. J.; Huard, M.; Cheng, H.; Mullen, M.; Ravuri, S.; Wang, B.; Wang, Y.; Huard, J., The use of heparin/polycation coacervate sustain release system to compare the bone regenerative potentials of 5 BMPs using a critical sized calvarial bone defect model. *Biomaterials* **2022,** 288, 121708.
19. Gao, X.; Lu, A.; Tang, Y.; Schneppendahl, J.; Liebowitz, A. B.; Scibetta, A. C.; Morris, E. R.; Cheng, H.; Huard, C.; Amra, S.; Wang, B.; Hall, M. A.; Lowe, W. R.; Huard, J., Influences of donor and host age on human muscle-derived stem cell-mediated bone regeneration. *Stem Cell Res Ther* **2018,** 9, (1), 316.
20. Turner, N. J.; Pezzone, M. A.; Brown, B. N.; Badylak, S. F., Quantitative multispectral imaging of Herovici's polychrome for the assessment of collagen content and tissue remodelling. *J Tissue Eng Regen Med* **2013,** 7, (2), 139-48.
21. Gao, X.; Usas, A.; Tang, Y.; Lu, A.; Tan, J.; Schneppendahl, J.; Kozemchak, A. M.; Wang, B.; Cummins, J. H.; Tuan, R. S.; Huard, J., A comparison of bone regeneration with human mesenchymal stem cells and muscle-derived stem cells and the critical role of BMP. *Biomaterials* **2014,** 35, (25), 6859-70.
22. Mannarino, M.; Cherif, H.; Ghazizadeh, S.; Martinez, O. W.; Sheng, K.; Cousineau, E.; Lee, S.; Millecamps, M.; Gao, C.; Gilbert, A.; Peirs, C.; Naeini, R. S.; Ouellet, J. A.; L, S. S.; Haglund, L., Senolytic treatment for low back pain. *Sci Adv* **2025,** 11, (11), eadr1719.
23. Deng, Z.; Gao, X.; Sun, X.; Amra, S.; Lu, A.; Cui, Y.; Eltzschig, H. K.; Lei, G.; Huard, J., Characterization of articular cartilage homeostasis and the mechanism of superior cartilage regeneration of MRL/MpJ mice. *FASEB J* **2019,** 33, (8), 8809-8821.
24. Utsunomiya, H.; Gao, X.; Cheng, H.; Deng, Z.; Nakama, G.; Mascarenhas, R.; Goldman, J. L.; Ravuri, S. K.; Arner, J. W.; Ruzbarsky, J. J.; Lowe, W. R.; Philippon, M. J.; Huard, J., Intra-articular Injection of Bevacizumab Enhances Bone Marrow Stimulation-Mediated Cartilage Repair in a Rabbit Osteochondral Defect Model. *Am J Sports Med* **2021,** 49, (7), 1871-1882.
25. Pritzker, K. P.; Gay, S.; Jimenez, S. A.; Ostergaard, K.; Pelletier, J. P.; Revell, P. A.; Salter, D.; van den Berg, W. B., Osteoarthritis cartilage histopathology: grading and staging. *Osteoarthritis Cartilage* **2006,** 14, (1), 13-29.
26. Stake, I. K.; Gao, X.; Huard, M.; Fukase, N.; Ruzbarsky, J. J.; Ravuri, S.; Layne, J. E.; Philippon, M. J.; Clanton, T. O.; Huard, J., Effects of Losartan and Fisetin on Microfracture-Mediated Cartilage Repair of Ankle Cartilage in a Rabbit Model. *Am J Sports Med* **2024,** 52, (14), 3625-3640.
27. Gillman, C. E.; Jayasuriya, A. C., FDA-approved bone grafts and bone graft substitute devices in bone regeneration. *Mater Sci Eng C Mater Biol Appl* **2021,** 130, 112466.

 doi:10.20944/preprints202604.0770.v1

28. Elangovan, S.; Khorsand, B.; Do, A. V.; Hong, L.; Dewerth, A.; Kormann, M.; Ross, R. D.; Sumner, D. R.; Allamargot, C.; Salem, A. K., Chemically modified RNA activated matrices enhance bone regeneration. *J Control Release* **2015,** 218, 22-8.
29. Surisaeng, T.; Wisitrasameewong, W.; Champaiboon, C.; Sa-Ard-Iam, N.; Chanamuangkon, T.; Thongnuek, P.; Tam, Y. K.; Muramatsu, H.; Weissman, D.; Pardi, N.; Pichyangkul, S.; Mahanonda, R., BMP-2 mRNA-transfected BMSCs promote superior calvarial bone regeneration. *Sci Rep* **2025,** 15, (1), 15022.
30. Khorsand, B.; Elangovan, S.; Hong, L.; Dewerth, A.; Kormann, M. S.; Salem, A. K., A Comparative Study of the Bone Regenerative Effect of Chemically Modified RNA Encoding BMP-2 or BMP-9. *AAPS J* **2017,** 19, (2), 438-446.
31. Balmayor, E. R.; Geiger, J. P.; Aneja, M. K.; Berezhanskyy, T.; Utzinger, M.; Mykhaylyk, O.; Rudolph, C.; Plank, C., Chemically modified RNA induces osteogenesis of stem cells and human tissue explants as well as accelerates bone healing in rats. *Biomaterials* **2016,** 87, 131-146.
32. Badieyan, Z. S.; Berezhanskyy, T.; Utzinger, M.; Aneja, M. K.; Emrich, D.; Erben, R.; Schuler, C.; Altpeter, P.; Ferizi, M.; Hasenpusch, G.; Rudolph, C.; Plank, C., Transcript-activated collagen matrix as sustained mRNA delivery system for bone regeneration. *J Control Release* **2016,** 239, 137-48.
33. Gao, X.; Usas, A.; Proto, J. D.; Lu, A.; Cummins, J. H.; Proctor, A.; Chen, C. W.; Huard, J., Role of donor and host cells in muscle-derived stem cell-mediated bone repair: differentiation vs. paracrine effects. *FASEB J* **2014,** 28, (8), 3792-809.
34. Aini, H.; Itaka, K.; Fujisawa, A.; Uchida, H.; Uchida, S.; Fukushima, S.; Kataoka, K.; Saito, T.; Chung, U. I.; Ohba, S., Messenger RNA delivery of a cartilage-anabolic transcription factor as a disease-modifying strategy for osteoarthritis treatment. *Sci Rep* **2016,** 6, 18743.
35. Pezzotti, G.; Zhu, W.; Terai, Y.; Marin, E.; Boschetto, F.; Kawamoto, K.; Itaka, K., Raman spectroscopic insight into osteoarthritic cartilage regeneration by mRNA therapeutics encoding cartilage-anabolic transcription factor Runx1. *Mater Today Bio* **2022,** 13, 100210.
36. Wu, H.; Peng, Z.; Xu, Y.; Sheng, Z.; Liu, Y.; Liao, Y.; Wang, Y.; Wen, Y.; Yi, J.; Xie, C.; Chen, X.; Hu, J.; Yan, B.; Wang, H.; Yao, X.; Fu, W.; Ouyang, H., Engineered adipose-derived stem cells with IGF-1-modified mRNA ameliorates osteoarthritis development. *Stem Cell Res Ther* **2022,** 13, (1), 19.
37. Huang, K.; Liu, X.; Qin, H.; Li, Y.; Zhu, J.; Yin, B.; Zheng, Q.; Zuo, C.; Cao, H.; Tong, Z.; Sun, Z., FGF18 encoding circular mRNA-LNP based on glycerolipid engineering of mesenchymal stem cells for efficient amelioration of osteoarthritis. *Biomater Sci* **2024,** 12, (17), 4427-4439.
38. Sun, M.; Ma, B.; Pan, Z.; Zhao, Y.; Tian, L.; Fan, Y.; Kong, W.; Wang, J.; Xu, B.; Ao, Y.; Guo, Q.; Wang, X.; Peng, X.; Li, X.; Cheng, J.; Miao, L.; Wang, K.; Hu, X., Targeted Therapy of Osteoarthritis via Intra-Articular Delivery of Lipid-Nanoparticle-Encapsulated Recombinant Human FGF18 mRNA. *Adv Healthc Mater* **2024,** 13, (29), e2400804.
39. Kong, K.; Li, B.; Chang, Y.; Zhao, C.; Qiao, H.; Jin, M.; Wu, X.; Fan, W.; Wang, L.; Qi, Y.; Xu, Y.; Zhai, Z.; Ma, P.; Li, H., Delivery of FGF18 using mRNA-LNP protects the cartilage against degeneration via alleviating chondrocyte senescence. *J Nanobiotechnology* **2025,** 23, (1), 34.
40. Fontana, G.; Nemke, B.; Lu, Y.; Chamberlain, C.; Lee, J. S.; Choe, J. A.; Jiao, H.; Nelson, M.; Amitrano, M.; Li, W. J.; Markel, M.; Murphy, W. L., Local delivery of TGF-beta1-mRNA decreases fibrosis in osteochondral defects. *Bioact Mater* **2025,** 45, 509-519.